

Spitzer Orbit Determination during In-Orbit Checkout Phase

Premkumar R. Menon*

Jet Propulsion Laboratory, California Institute of Technology, Pasadena, CA 91109-8099

The Spitzer Space Telescope was injected into heliocentric orbit on August 25, 2003 to observe and study astrophysical phenomena in the infrared range of frequencies. The initial 60 days was dedicated to Spitzer's "In-Orbit Checkout (IOC)" efforts. During this time high levels of Helium venting were used to cool down the telescope. Attitude control was done using reaction wheels, which in turn were de-saturated using cold gas Nitrogen thrusting. Dense tracking data (nearly continuous) by the Deep Space network (DSN) were used to perform orbit determination and to assess any possible venting imbalance. Only Doppler data were available for navigation. This paper deals with navigation efforts during the IOC phase. It includes Dust Cover Ejection (DCE) monitoring, orbit determination strategy validation & results and assessment of non-gravitational accelerations acting on Spitzer including that due to possible imbalance in Helium venting.

I. Introduction

The Space Infrared Telescope Facility (SIRTF) as it was initially called, was launched into space on August 25, 2003 from Cape Canaveral using a Boeing Delta II 7920H-9.5 launch vehicle. It was injected into an Earth-trailing heliocentric orbit (Fig. 1) to facilitate observing various astrophysical phenomena in the infrared range of frequencies. Keeping the tradition of renaming the "Great Observatories" after launch, SIRTF too was renamed in honor of a great American scientist. Thus on December 18, 2003, SIRTF acquired the new name Spitzer Space Telescope ("Spitzer" in short) after Dr. Lyman Spitzer who made pioneering efforts to put telescopes in space.

The Spitzer team consists of the National Aeronautics and Space Administration (NASA), the Jet Propulsion Laboratory (JPL), Spitzer Science Center at California Institute of Technology, Ball Aerospace and Technologies Corporation, Lockheed Martin Space System Company, Smithsonian Astrophysical Observatory, Cornell University, and University of Arizona. Spitzer is a space-borne, cryogenically cooled infrared observatory capable of studying objects ranging from our Solar System to the distant reaches of the Universe and is intended for the science community to observe & analyze the astrophysical phenomena in the infrared range of frequencies. It is the last of the four NASA "Great Observatories", the other 3 being Hubble Space Telescope (HST), Compton Gamma-Ray Observatory (CGRO) and Chandra X-Ray Observatory (CXO).

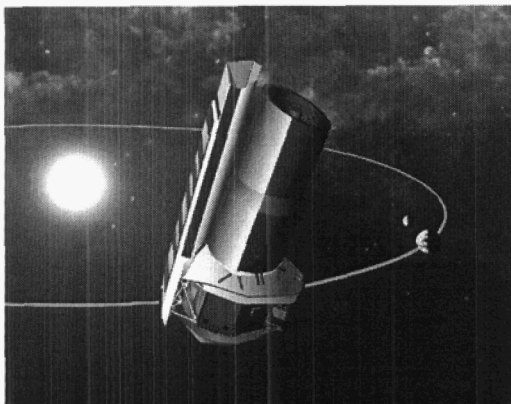


Figure 1. Artist Interpretation of Spitzer in Earth-trailing heliocentric orbit

It is the last of the four NASA "Great Observatories", the other 3 being Hubble Space Telescope (HST), Compton Gamma-Ray Observatory (CGRO) and Chandra X-Ray Observatory (CXO).

Spitzer was injected into a heliocentric orbit with an injection-energy, C_3 of $0.393 \text{ km}^2/\text{s}^2$ (nominal $C_3 = 0.40 \text{ km}^2/\text{s}^2$). It trails the Earth, drifting away at an average rate of about 0.124 AU per year (0.59 km/s). Figure 2 shows Spitzer's trajectory in the Sun-Earth rotating frame. Two consecutive loops require 1 year to complete. Being away from the Earth helps prevent heating due to re-radiation. The different phases of the mission are also color-coded Fig. 2. The primary mission lasts for about 2.5 years and the current estimates allow the mission-goal of about 5+ years life span to be met. The In-Orbit Check out (IOC) Phase spanning the initial 60 days was dedicated to checking out on-board engineering systems and was followed by 30 days of Science Verification Phase. The Navigation Activity during different phases of the mission is given below in Table 1.

* Member of Engineering Staff, Navigation and Mission Design Section, Jet Propulsion Laboratory, 4800 Oak Grove Drive, MS 301-125J, Pasadena, CA-91109-8099, premkumar.menon@jpl.nasa.gov

Table 1. Mission Phases and navigation activity

<i>Mission Phase</i>	<i>Time-span</i>	<i>Navigation Activity</i>
In-Orbit Checkout (IOC) Phase	Launch to L+60d	Initial Acquisition Support / Venting Verification Tests / Orbit Solution Generation
Science Verification (SV) Phase	L+60d to L+90d	Weekly Orbit Determination
Primary Mission Phase	L+90d to L+2.5y	" "
Extended Mission Phase	L+2.5y to 5y	" "

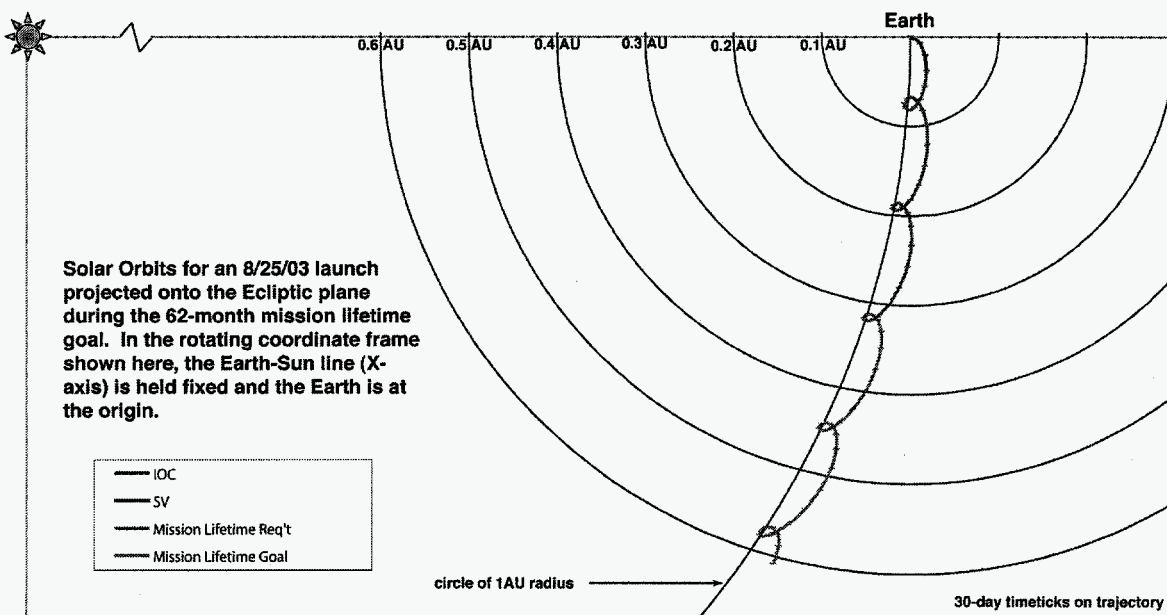


Figure 2. Spitzer in heliocentric orbit (Launch to L+62 months)

The Spitzer Space telescope was launched “warm” and was cooled down during the initial few weeks of the mission to near 5.5 degrees Kelvin and thereafter maintained at steady state low levels of temperature using cryogenic liquid Helium venting. Communication with the ground stations is through the spacecraft high-gain antenna except during the early part of the IOC phase when low-gain antennae (LGA-s) were used. The Reaction Control System (RCS) is a cold gas system and uses Nitrogen as the propellant.

Only Doppler data was available to perform orbit determination of the Spitzer Space Telescope. Tracking coverage was very dense (nearly continuous) during the IOC period. Navigation tasks included orbit determination as well as efforts to assess non-gravitational accelerations acting on the observatory, especially that due to any possible imbalance in Helium venting. Tests were planned and executed to assess the above during high venting activity as well as at lower levels. The spacecraft was maintained in different attitudes during tracking in order to achieve observability of venting effects in the three spacecraft axes. This is described in detail later.

Estimation strategy included solving for the spacecraft state, the angular momentum de-saturation (AMD) maneuvers, and stochastic accelerations. The stochastic accelerations that were estimated included any mis-modeling of solar radiation pressure, possible venting imbalance, possible RCS thruster leaks, etc. The results

indicate that acceleration due to venting in each spacecraft axis is lower than the pre-launch worst-case prediction. The trajectory was propagated forward using converged orbit solution and new data passed through to test the fidelity of the orbit determination process. Orbit determination results indicate that the navigation requirements are also easily satisfied.

II. Observatory Description

The Spitzer observatory consists of a 0.85meter telescope, three science instruments and the spacecraft bus (Figure 3). The Infrared Array Camera (IRAC) is a four-channel imager with simultaneous viewing at 3.4, 4.5, 6.3 and 8.0 microns. The Multi-band Infrared Photometer for SIRTf (MIPS) has five distinct optical trains that can image simultaneously at 24, 70 and 160 microns, or obtain low-resolution spectra from 50 to 100 microns. The Infrared Spectrograph (IRS) has four separate optical trains that cover the spectral range from 5 to 40 microns. The telescope is protected from the sun by a solar panel shield upon which solar panels are attached. The spacecraft houses the electronics, Low Gain Antennae, High Gain Antenna, Star Tracker & Inertial Reference Units, Reaction Reference Units, Reaction Control System Thrusters, etc. The high gain antenna (HGA) is situated in the $-X$ side (opposite direction from the telescope bore-sight). The LGA-s are located on both the $+Y$ and $-Y$ sides of the spacecraft bus. The high gain antenna is canted 8° in order to aid Earth-acquisition during the early part of the mission. The dust cover (not shown in Figure 3) was ejected 4 days after the commencement of the mission in order to allow light into the telescope. The Spacecraft Shield between the spacecraft bus and the Cryostat Telescope Assembly (CTA) minimizes the radiative heat transfer from the spacecraft bus to the cryostat. The Outer Shell of the CTA is painted silver on the side facing the Solar Panel Shield so that it reflects heat imparted from the sun-side components, while the backside of the outer shell (which always faces the deep space) is painted black for maximum radiation. The Reaction Control System (RCS) De-saturation thrusters, Cryogenics Helium Venting System and surfaces affected by solar radiation pressure acceleration are discussed in more detail later. The launch mass for the Observatory was 851.5 kg, for Dust Cover 6.4 kg, for Helium 50.4 kg and for Nitrogen Propellant 15.6 kg.

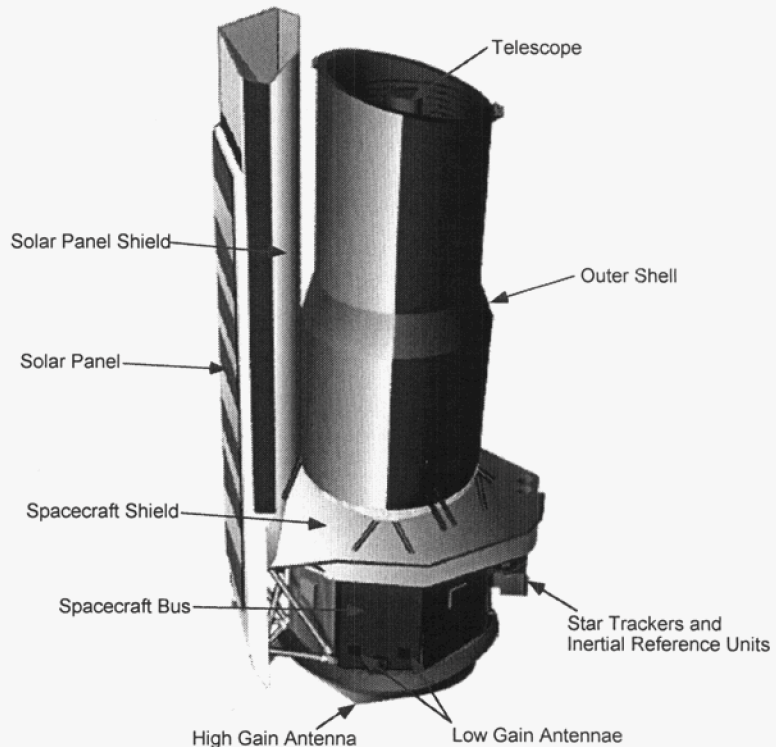


Figure 3. Spitzer Observatory

III. Spitzer trajectory & operating constraints

During normal operations, the S/C will be able to point the telescope bore-sight anywhere within the viewing constraints depicted in Figure 4. Staying within the viewing constraints is necessary to generate adequate solar power and to protect the CTA from the heating effects of direct solar illumination. Pointing the telescope bore-sight within 80° of the Sun causes direct solar illumination of the telescope barrel, which could permanently damage the instruments. This was changed to 82.5° after the IOC in order to maintain health & safety while increasing observational efficiency. Pointing the telescope bore-sight more than 120 degrees from the Sun causes an unacceptable degradation of the solar array performance. The result of these constraints is an annulus-shaped "operational pointing zone" or OPZ that rotates as the Observatory revolves around the Sun. Targets near the ecliptic pole within the "constant viewing zone" or CVZ are always viewable; targets near the ecliptic plane are viewable every six months for a period of at least 40 days. The telescope bore-sight is also allowed to roll $\pm 2^\circ$ about the optic axis (X-axis), otherwise the sunlight striking the outer shell could permanently damage its thermal

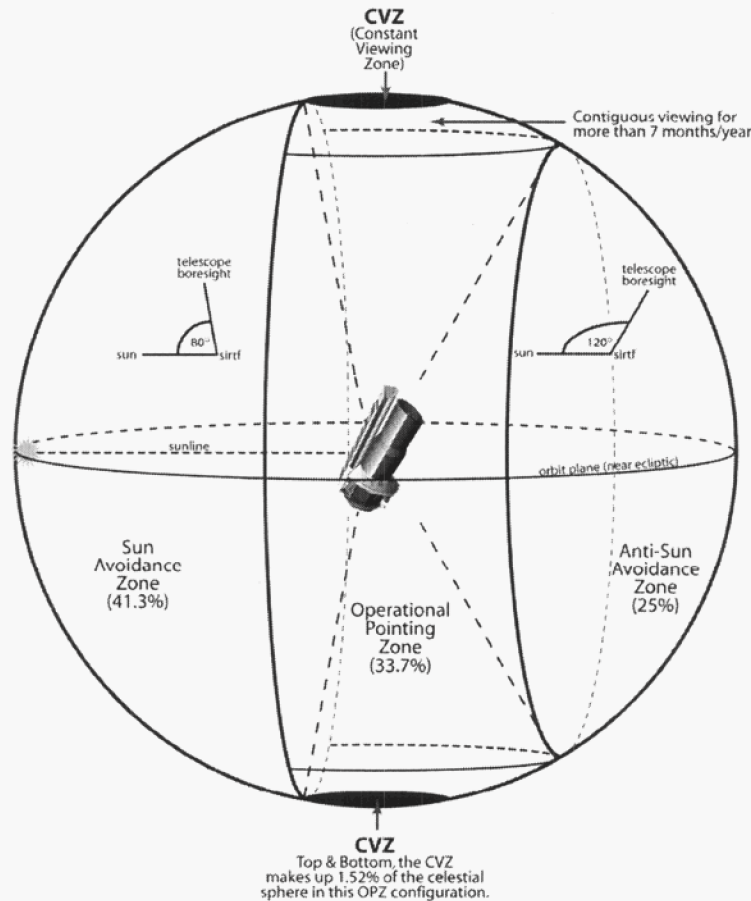


Figure 4. Spitzer Operational Zone

properties. Thus Spitzer's observation sequence drives its attitude history, which in turn dictates the strategy used to model the non-gravitational accelerations. Information about the observatory attitude as a function of time is obtained from the C-Kernel generated from the Spitzer telemetry and utilized in the orbit determination process.

IV. In-Orbit Checkout Phase

The In Orbit Checkout (IOC) phase spanned the initial 60 days. During the first week the on-board ephemeris was updated at about L+36hours and then about L+4.5days. Further updates were done weekly, thereafter. The momentum dumps during the first few days were very frequent due to vigorous boil-off from the Helium tank. These momentum dumps were done autonomously. Other mission critical events during this phase included dust cover ejection (L+4.7days) and a perture door opening (L+5.7days). Various calibration, checks and evaluations were done during IOC. The Helium mass measurement was done after about 60days. Momentum dumps are now routinely executed during down link sessions.

A. Dust Cover Ejection

In-Orbit Checkout phase commenced about 4 hours after lift-off. On the 4th day the dust cover was ejected in order to expose the telescope. The predicted relative velocity between the dust cover and Spitzer observatory was 0.98 ± 0.02 m/s. Spitzer, though significantly more massive than the dust cover was expected to recoil with a small delta-V resulting from the ejection. The component of this delta-V in the line of sight from the Goldstone tracking station resulted in the 2-way Doppler data residuals (Observed - Predicted frequency) being observed in real-time, aiding confirmation of the ejection. The expected shift along the line-of-sight was 0.2hz (~3.6mm/s). The actual observed shift in the 2-way Doppler data residual was about 0.217hz (~3.9mm/s) as seen in figure 5. The first residual shift seen in figure 5 is due to Angular Momentum De-saturation Maneuver prior to the ejection. The second jump in residuals resulted from the actual ejection of the dust cover itself. The trajectory of the dust cover has also been propagated.¹

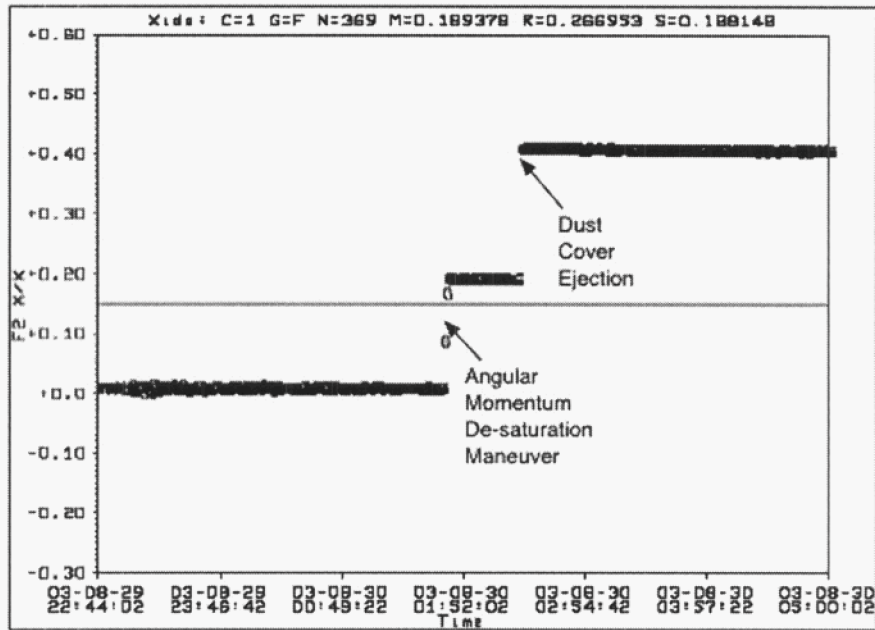


Figure 5. 2-way Doppler residual display during dust cover ejection period
X-axis indicates date & time, Y-axis shows data residuals in hertz.

B. Venting Verification Tests

During the first 60 days (In-Orbit Checkout Phase), Spitzer tracking by the DSN was nearly continuous. The Navigation team had planned to take advantage of this dense tracking schedule to analyze Spitzer's venting behavior. The cryogenic Helium venting was expected to be balanced and along the +Y and -Y axes of the spacecraft. However, assumption of a 5% error in Helium flow rate predicted a worst-case net acceleration on Spitzer.² Venting levels varied within the IOC period due to cooling down of the telescope. This is shown below in Table 2.

Table 2. Predicted Net Acceleration due to Helium Venting (5% Flow Division Error)

Time Span	Test Dates (Days from launch)		Predicted Worst-Case Net Acceleration (km/s ²)	Comments
	Planned	Actual		
Launch to L+1.5d			3.05×10^{-10}	Initial Acq./Safe mode
L+1.5d to L+5d	2		3.63×10^{-10}	Maximum Thrust
L+5d to L+10d	5	7, 9	3.24×10^{-10}	Intermediate Levels
L+10d to L+20d	11	16	9.28×10^{-11}	Intermediate Levels
L+20d to L+35d	22	28	3.61×10^{-11}	Low Levels
L+35d to L+1830d	35	Unlabeled	$3.63 \text{ to } 3.93 \times 10^{-12}$	Steady State

In order to assess venting behavior during these segments, venting verification tests were proposed to the project. After approval from the Mission Change Request Board, these tests were included in the IOC-activities.³ Potential dates were selected in order to utilize different levels of venting, such as high level venting, medium level venting and steady state (low level) venting periods. Tests were carefully planned to avoid conflicts with other important IOC activities. This led to scheduling tests at 2, 5, 11, 22 & 35 days after launch. However, Spitzer went into safe-mode early in the mission (launch day) and thereby changes in the new schedule dictated venting test dates to be updated to 7, 9, 16, 28 and 37 days after launch. The early results after the first two tests indicated that the non-gravitational acceleration (including any venting imbalance) was very small indicating insignificant venting imbalance. This determination and subsequent test results led to the eventual decision to cancel the 5th test (day 37) making room for high priority IOC activities.

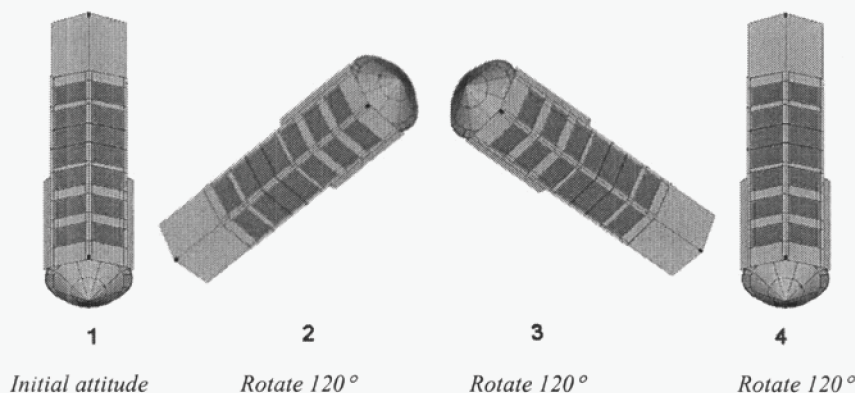


Figure 6. Venting Verification Test Attitudes.

Test definition was to initially maintain the Spitzer observatory for 2 hours at an attitude with the Z-axis (normal to the solar panels) towards the Sun. It is to be then rotated about Sun-line by about 120° and maintained at the new attitude for another 2 hours. Again, it is to be rotated in the same direction by 120° about the Sun-line and maintained at the 3rd attitude for 2 hours. Finally it is to be rotated in the same direction for another 120° and brought back to the initial attitude and maintained for 2 hours. The different attitudes as seen from the Sun are shown in figure 6. By turning & holding at these attitudes non-gravitational accelerations in all three directions could be detected and any significant venting imbalance especially in the spacecraft Y-direction noted. During these tests, communication with Spitzer was through its low-gain antenna acquiring 2-way Doppler tracking data.

1. Cryogenic Helium Venting

The primary goal of these tests was to verify the navigation strategy in dealing with the Helium venting effects. The venting might be either strictly stochastic (random) or might exhibit systematic trends in size and direction. The tests were complicated by other factors. Acceleration due to solar radiation pressure affected Spitzer mostly along the Z-axis (normal to the solar panels) and somewhat along the X-axis (along telescope bore-sight). The Angular Momentum Desaturation maneuver could be in any direction. Errors in these estimates and/or gas leaks could also alias the venting acceleration. Since it was impossible to decouple these effects, net non-gravitational acceleration

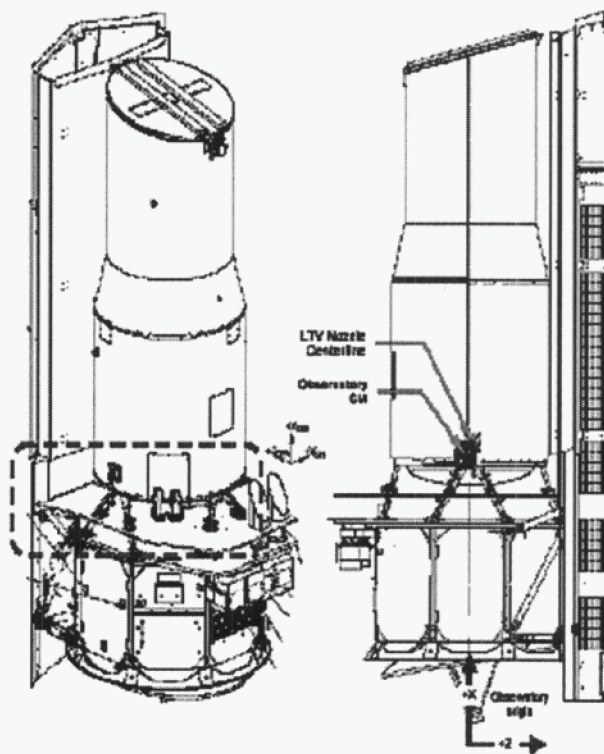


Figure 7. Spitzer Cryogenic Venting System.

with contributions from all the above were estimated. Since venting was expected to be in the Y-direction (out of the paper, figure 7 right-hand side) and since solar pressure had the least effect in this direction, only any mis-modeling in AMD and or possible thruster leaks, could corrupt the estimates in this direction.

2. Angular Momentum De-saturation

The Spitzer Reaction Control System (RCS) is a cold gas system that uses Nitrogen as propellant. The project plans called for de-saturation burns about every 1 to 1.5 days during the nominal mission to unload the momentum and maintain the reaction wheel rates within operational specs. During steady state (Routine phase) the ΔV predicted from these dumps ranged from 6.2 to 6.7 mm/s (Ref. 2), assuming a 6.0 N-m-s reduction in momentum. The worst case in thruster leaks was expected to contribute an impulse of about 0.4 N-s every 36 hours.⁴ It had to be taken into account during orbit determination. During early IOC, momentum de-saturation operations were to occur more often (every few hours) due to increased venting from the CTA. The first possible momentum dump would occur just after launch vehicle separation. The size of the dump was determined by the tip-off rates imparted by

the launch vehicle. A 3σ tip-off rate would impart 30 Nms of momentum to the Observatory, resulting in a dump of 29 Nms of momentum upon PCS activation.²

The location and orientation of the thrusters are shown in figure 8. The magnitude and directions of the ΔV s were available to the Navigation team via Angular Momentum De-saturation Delta-V Data file (OIA-NAV-04).⁵ The 1σ accuracy in magnitude of this reconstructed ΔV was expected to be 1.0 mm/s.⁶ The direction had an uncertainty of 10° and was given in J2000 ICRS coordinates.

There are 12 thrusters available to de-saturate the angular momentum build-up of the reaction wheels. Each of the 6 co-located pairs includes a primary and a backup thruster. Thrusters 5, 6, 11 & 12 are in the XZ plane and canted 32° with respect to the +Z axis. Thrusters 1, 4, 7 & 10 are oriented to make 30° with the Y-axis and were in the XY plane. However, thrusters 2, 3, 8 & 9 in the YZ plane are not canted and point in the -Z direction.

3. Solar Radiation pressure

Solar radiation pressure was modeled by assuming that the only surfaces directly illuminated were the solar panels and a small area of the radome covering the HGA. Figure 9. shows these surfaces, their absorptivity (α) and emissivity (ϵ) when the solar cells are in their active (closed circuit) mode. Strings of cells are open circuited when the power is not needed for spacecraft and instrument operations. In the open circuit configuration, the solar absorptivity goes up by the electrical conversion efficiency of the

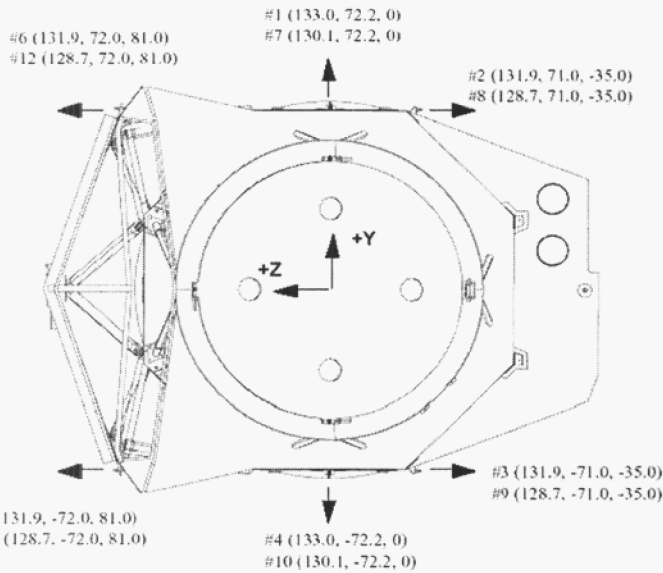


Figure 8. R Reaction Control System thruster locations.

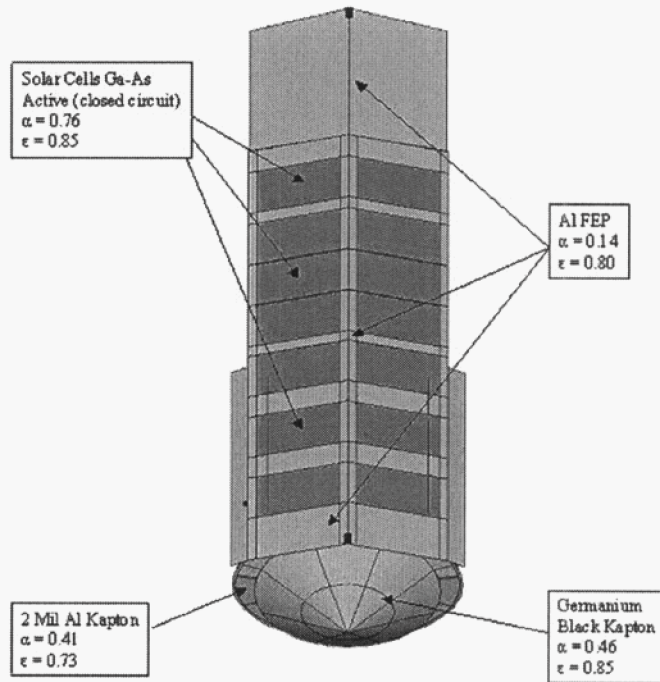


Figure 9. Surfaces exposed to solar radiation.

cells. Electrical power system models predicted approximately 5 strings active early in the mission with more strings added as the cell efficiency degrades or as mission operations require. The solar cells have cover glass that acts as a band pass filter for wavelengths between 0.35 μ m and 1.1 μ m. All incident solar flux outside that band is 100% specularly reflected. A large percentage of the solar panel is covered with aluminized Teflon Flexible Optical Solar Reflector (FOSR) as shown in Fig. 9.⁷ In addition, the original solar pressure model assumed a beta cloth cover for the high gain antenna, whereas the actual design used a single layer of germanium black Kapton.

To simplify the solar pressure model, a Flat Plate model was used to represent the two segments of the solar

Table 3. Parameters to model acceleration due to solar radiation pressure.

Component (1-sided flat plate)	Area (m ²)	Reflectivity Coefficient		Direction
		Specular	Diffuse	
Solar Panel# 1	3.274	0.282	0.124	19° from +Z toward +Y
Solar Panel# 2	3.274	0.282	0.124	19° from +Z toward -Y
HGA Radome Cover	1.961	0.265	0.131	-X

panel (+/-19° off from +Z direction). Each of these flat plates has an area of 3.274m² and average values of the solar pressure parameters. Solar cells constitute about 46% of the total area of the solar panel and Aluminum Teflon make up the rest. Hence the parameters were averaged accordingly. A flat plate model with an area of 1.961m² was used to represent the radome cover in the -X direction. The area, orientation, specular & diffuse reflectivity coefficients of each component are shown in Table 3. The net nominal acceleration due to solar radiation pressure ranged from 5.5 to 5.8 x 10⁻¹¹ km/sec². Uncertainty in the solar pressure model was a key contributor to the orbit determination error. The orientation of Spitzer is continuously changing throughout the observation sessions, which causes the area illuminated by the sun to change, thus making it difficult to predict the orientation and the effective area. The uncertainty in the orientation combined with the error in the reflectivity coefficients was treated as an additional stochastic acceleration.

C. Orbit Determination

1. Navigation Requirements

In the absence of any Science requirement, the Navigation requirements were expressed as antenna pointing, velocity (frequency) predicts and accuracy in one-way light time as shown in Table 4. The most stringent pointing requirement was based on acquisition by the DSN 70-meter station. Also, the Observatory Engineering Team (OET) needed a One-way light time accuracy of 6 milliseconds with a goal of 2 milliseconds.⁸

Table 4. Navigation Requirements.

Parameter	Requirement (1 σ)	Driven By
Position	1800 km	One-way light-time accuracy 6 ms (goal 2ms)
Velocity	70 m/s	Frequency Predicts
Angle	0.015° (70M) 0.066° (34M)	Pointing Predicts

2. Estimation Strategy

A batch sequential filter was used to perform orbit determination. The converged solution was then used to generate the predicted trajectory. The filter treated the venting and solar pressure errors as dynamic stochastic error sources modeled by a Gauss-Markov process. The batch sequential filter assumed a fixed batch size for the solar

Table 5. Estimated Parameters and a priori uncertainties.

PARAMETER	UNCERTAINTY (1σ)	COMMENTS
Constant Parameters Position Velocity Angular Momentum Desats.	1,000 km 0.1 km/s $2 \times 10^{-7} \text{ km/s}^2$	Epoch State
Stochastic Parameters Acceleration from Venting + Gas leaks + SRP model error	$3 \times 10^{-10} \text{ km/s}^2$ $3 \times 10^{-11} \text{ km/s}^2$ (after 9/22)	10d batch, white noise
Consider Parameters Troposphere Dry Zenith Component Wet Zenith Component Ionosphere Day Night	1 cm 4 cm 75 cm 15 cm	

pressure and venting errors with appropriate correlation time. The momentum unloading maneuvers were estimated. An X-band Doppler data weight of 0.1 mm/sec was assumed for a 60 second count time. In addition, the media errors were also considered. Table 5 summarizes the parameters that were estimated along with the a priori and consider error assumptions. Since venting levels came down to nearly steady state (after a month from launch), the a-priori uncertainty for the non-gravitational acceleration were lowered by an order of magnitude from the earlier levels.

Attitude history information acquired from the Spitzer telemetry was used to model its orientation thereby improving the solar pressure effects. Only a minimum number of parameters were solved in order to reduce the possibility of a liasing into venting estimates. Parameters included the observatory state and the momentum desaturation maneuvers. The non-gravitational accelerations were estimated stochastically as stated above and were isolated during each test. Only 2-way Doppler data were available.

C. Results

The orbit determination results from the venting verification tests are given below. Plots showing the non-gravitational acceleration (Spitzer-fixed coordinates) estimates along with error bars are illustrated in figure 10. Since most of the error bars are barely visible, Table 6 may be referenced for clarity. As can be seen, the earlier acceleration estimates were higher than in the later steady state areas. This may be attributed to higher venting

Table 6. Estimated Non-Gravitational Acceleration and 1σ Uncertainty.

Case	Estimated Acceleration & 1σ Uncertainty (km/s ²)					
	X		Y		Z	
	Value	1σ	Value	1σ	Value	1σ
<i>Test# 1</i> (L+7d)	-1.92×10^{-11}	2.22×10^{-12}	1.40×10^{-11}	4.21×10^{-13}	-2.21×10^{-11}	8.96×10^{-13}
<i>Test# 2</i> (L+9d)	-9.70×10^{-11}	2.53×10^{-12}	1.88×10^{-11}	1.22×10^{-13}	-1.26×10^{-11}	2.44×10^{-13}
<i>Test# 3</i> (L+16d)	-1.27×10^{-12}	9.86×10^{-14}	-6.09×10^{-13}	5.35×10^{-14}	1.93×10^{-12}	7.68×10^{-14}
<i>Test# 4</i> (L+28d)	1.15×10^{-12}	1.34×10^{-13}	1.44×10^{-12}	1.96×10^{-13}	2.63×10^{-12}	1.39×10^{-13}
<i>Constant Acceleration</i>	1.03×10^{-12}	3.84×10^{-14}	1.59×10^{-12}	9.12×10^{-14}	2.75×10^{-12}	5.45×10^{-14}

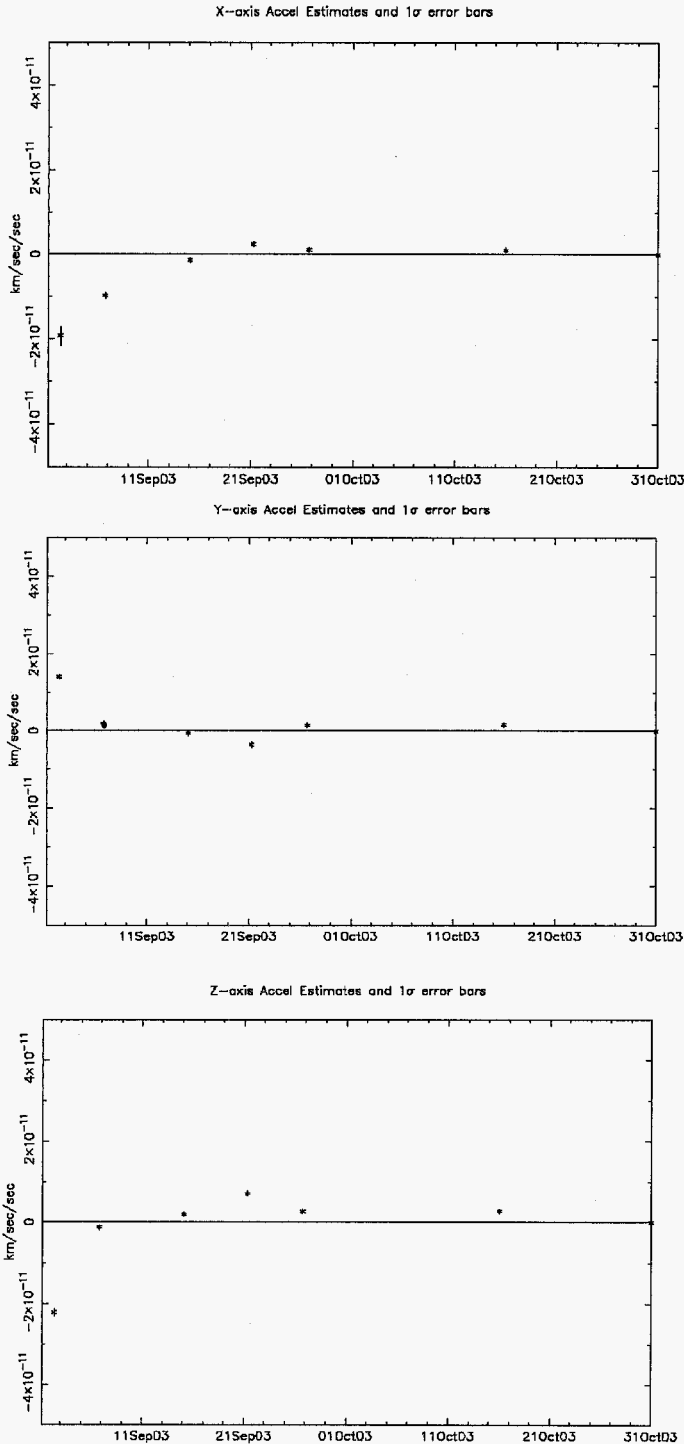


Figure 10. Non-gravitational acceleration and 1 σ -error bars in Spitzer X, Y, Z axes Vs. Time.

activity during earlier periods and thereby more frequent Angular Momentum desaturation maneuvers estimates, which weakened the data. Table 6 gives the estimates and their associated 1 σ -uncertainties. Constant acceleration estimated using about 30 days of tracking data is given in the last row. The tests 1-4 correspond to the 1st, 2nd, 3rd and 5th data points in the plots. The results indicate that the non-gravitational accelerations were well below the pre-launch prediction (worst-case) for the venting imbalance. Acceleration stochastically estimated from the 4th test was consistent with the constant acceleration estimated using 30 days of tracking data. The acceleration along the Y-axis was nearly half that from the pre-launch prediction. Since the Helium venting was expected to be along the +Y & -Y axes, this implied that venting imbalance was nearly zero during steady state low venting period. The other two directions, especially Z-axis might have errors from solar pressure mis-modeling and possible RCS thruster leaks.

How well the determined orbit could propagate was also assessed. This is illustrated in figure 11. The orbit was predicted for 2 weeks beyond the data cutoff and the new tracking data passed through it. As can be seen at the end of predicted 2 weeks the Doppler residual offset is about 1.7hz, which corresponds to a position offset of about 37km in the line of sight. This is well within the navigation capability of 80km (for the near Earth phase of the mission) predicted by the post-launch update of the Navigation Covariance analysis.⁹ Also, this easily meets the 6 milliseconds (1800 km) requirement and even 2 milliseconds (600 km) goal.

However, it is to be noted that navigation covariance analysis has shown that the orbit estimates resulting from using tracking data during low declination (below 5 $^\circ$) periods and at maximum distances have yielded higher uncertainties. Yet, these uncertainties were still low enough to meet the requirements.

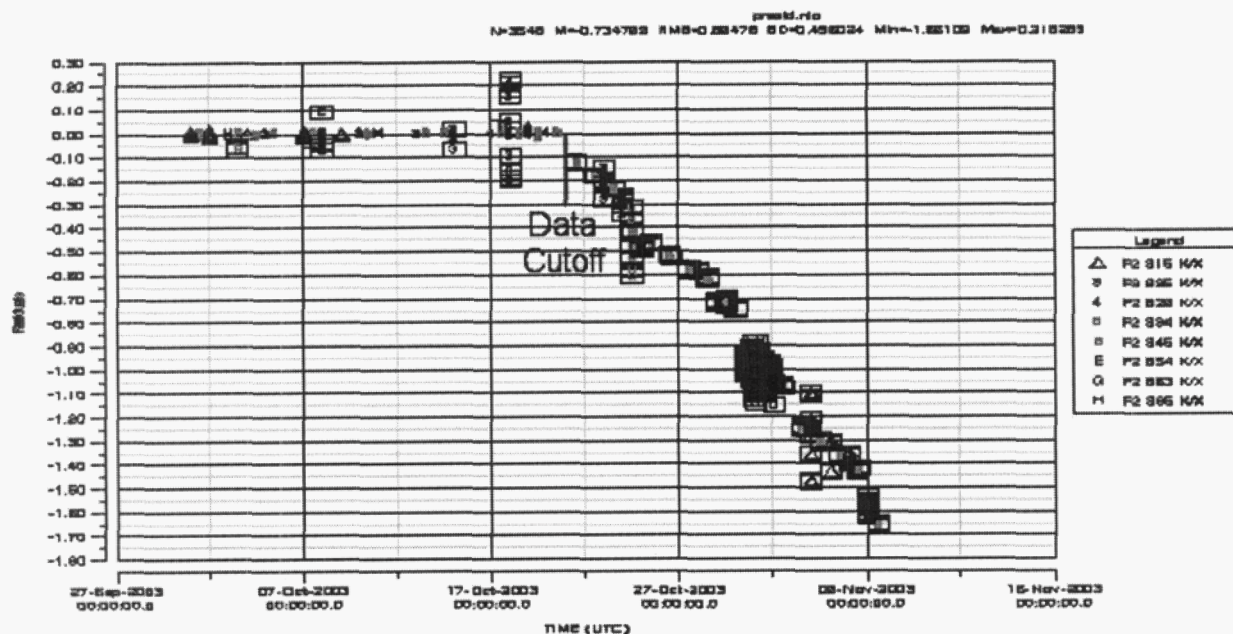


Figure 11. Reconstructed and Predicted Data Residuals (Hz) Vs. Time.

V. Conclusion

In conclusion, the non-gravitational accelerations were well below the worst-case predicted levels of acceleration. It was impossible to decouple effects due to solar pressure & potential RCS thruster leaks from venting. However, since the venting was along the Y-axis and since the Spitzer OPZ restricts SRP acceleration to be mostly along -Z (and somewhat along the X directions) one can assume that Y acceleration to be mostly due to the venting contribution. This being about half of the pre-launch prediction gave a “warm-fuzzy” feeling about the near-zero imbalance in Helium venting. If there had been significant imbalance, it would have manifested as a bias in the non-gravitational acceleration (especially in the Y-direction). This estimated bias could be accounted for in the trajectory propagation as well. The predicted trajectory was well within the Navigation capability and requirement.

Acknowledgments

This research was carried out at the Jet Propulsion Laboratory, California Institute of Technology, under a contract with the National Aeronautics and Space Administration. The author thanks Joseph Guinn & Timothy McElrath for their guidance in this work. The author also thanks Mark Garcia (Spitzer Mission Design Engineer) for the valuable suggestions. The help with the figures by Julie Evans is gratefully acknowledged. Colleagues who reviewed this paper are also appreciated. Above all, the author wishes to dedicate this work to the fond memory of Dr. Glenda L. Vittimberga who was a source of immense inspiration.

References

- ¹Garcia, M. D., “SIRTF Takes Flight,” Paper AAS 04-225, Honolulu, HI, Feb 16-20, 2004.
- ²Day, J., “Small Forces Determination on SIRTF,” SIRTF Engineering Memo. (14-May-2002), revised Aug 29, 2002.
- ³Menon, P. R., “Venting Characterization Tests,” JPL MMO Mission Change Request# 1847, approved May 5, 2003.
- ⁴Dodder, R. (LMA Sunnyvale), Telephone Conversation, July 29, 2002.
- ⁵Menon, P. R., “SIRTF Angular Momentum De-saturation Delta-V data,” OIA-MMNAV-04, Feb 26, 2003 <http://sirtfweb.jpl.nasa.gov/STAR.html>
- ⁶Day, J., “Momentum dump delta-V accuracy,” E-mail to D. Swanson & J. Tietz, Nov 4, 2002.
- ⁷Dempsey, B. and Yanari, C., “Data for Solar Pressure Model,” LMA Engineering Memo# TCS-027, August 5, 2002.
- ⁸Barry, S., “SIRTF Ground Systems Requirements, 674-MO-100, Requirement# 3.2.48,” May 5, 2003 http://sirtfweb.jpl.nasa.gov/inv/MOS/MOSSysEngrg/MOSSysEngDocs/MOS_Rqts_final.pdf.
- ⁹Menon, P. R., “SIRTF Initial Orbit Navigation Performance,” JPL Presentation Package, Nov 14, 2003.